

UNSTEADY FLOW FIELD MEASUREMENTS IN AN INDUSTRIAL CENTRIFUGAL COMPRESSOR

by

Lorenzo Toni

Engineer

Valeria Ballarini

Test Data Analysis & Advanced Instrumentation Technologist

Stefano Cioncolini

Principal Engineer

GE Oil & Gas

Firenze, Italy

Paolo Gaetani

Assistant Professor

and

Giacomo Persico

Assistant Professor

Politecnico di Milano

Milano, Italy



Lorenzo Toni is an Engineer in the Advanced Technology Division of GE Oil & Gas, in Florence, Italy. His primary role is experimental activities related to centrifugal compressors; he is responsible for advanced instrumentation and measurement techniques as well as data acquisition, analysis, and post-processing.

Dr. Toni received his M.S. degree (Mechanical Engineering, 2005) from the University of Florence and his Ph.D. degree (Energy Engineering, 2009), with a doctoral thesis on "Gas Turbine Aero-Engines Effusion Cooling Systems," from the same institute. He is the author or coauthor of several technical papers in the field of turbomachinery.



Stefano Cioncolini has filled the role of Principal Engineer in the Oil & Gas Technology Laboratory of GE Oil & Gas, in Florence, Italy, since 2008. Since 2005 he has led the Test Data Analysis group. His main activities are research and development of advanced measure methodologies and techniques for the validation of turbomachinery performance.

Dr. Cioncolini graduated with a degree (Physics, 1992). Since 1997, he has worked in the Advanced Technology Division Technology Laboratory of GE Oil & Gas.



Valeria Ballarini is a Test Data Analysis & Advanced Instrumentation Technologist for centrifugal compressor model tests, with GE Oil & Gas, In Florence, Italy. Her main research interests are: development of tools for data acquisition and post processing; development of sensors and acquisition hardware for thermodynamic measurements; and development of methods for the calculation of uncertainty in measurement

chains. She has been working in the Advanced Technology Laboratory since 2006.

Dr. Ballarini graduated (Materials Science, 2001) from the University of Torino. She received a Ph.D. degree (Physics) from Polytechnic of Torino with a thesis on "Growth and Characterization of Semiconductor/Insulating Films and Nanostructures for Electronic and Photonic Applications." Dr. Ballarini is the coauthor of more than 10 papers in international peer-reviewed journals.



Paolo Gaetani has been an Assistant Professor at the Politecnico di Milano, in Milan, Italy, since 2001. During this time he has designed and developed fast response aerodynamic pressure probes that have been successfully applied to the investigation of blade row interaction phenomena in modern axial turbines and centrifugal compressors. At the present time he is responsible for the Turbine-Compressor

Test Rig located at the Politecnico di Milano. He has also collaborated on inter-university and industrial research programs focused on the design and optimization of turbomachinery components and measurement techniques, the latter also being suitable for dense gas applications.

Dr. Gaetani graduated (Mechanical Engineering, 1993) from the Politecnico di Milano, and earned a Ph.D. degree (Energetics, 1997) from the same University. From 1997 to 2001 he had a research grant aimed at developing measurement techniques and test rigs for the study of blade row interaction phenomena.



Giacomo Persico is presently an Assistant Professor at Politecnico di Milano, where he teaches Fluid-Machine courses. His main research interests are the interaction of blade rows in turbomachinery, the development of fast-response measurement techniques, CFD applications, and through-flow methods. He is the author of about 30 papers that have been presented at international conferences or published in technical journals.

Dr. Persico graduated (Mechanical Engineering, 2002) from Politecnico di Milano, where he also earned a Ph.D. degree in 2006. He was a visiting doctoral candidate and then a visiting researcher at the Von Karman Institute for Fluid Dynamics in 2005-2006, and then a visiting scientist at the Graz Technical University in February 2007.

ABSTRACT

Unsteady flow field measurements of both static and total pressure, and discharge angle have been carried out downstream of an industrial centrifugal impeller. Phase-resolved measurements were performed using a cylindrical single sensor fast response aerodynamic pressure probe (FRAPP) traversing and rotating from the impeller hub up to the shroud. Since FRAPP operates as a virtual three-hole probe, it was possible to obtain a detailed bidimensional reconstruction of the flow field.

An experimental campaign was conducted on a closed loop rotating rig, where a multistage compressor was replicated using a pseudostage just upstream of the impeller to be tested, which was purposely designed for oil and gas applications. By varying the flow coefficient along a speed line, flow field modifications with pressure ratio variations were highlighted and analyzed in detail.

The results are presented as bidimensional distributions of total and static pressure as well as blade to blade angle (i.e., the angle in the plane normal to the probe axis) and Mach number; hub-to-shroud profiles and mass averaged data of the most significant quantities are also shown.

Moreover the typical pulsating behavior of centrifugal impellers, also known as the jet and wake phenomenon, has been captured and verified against standard pneumatic pressure probes (such as multihole probes) that in some cases evidence a lack of reliability. A comparison of these different techniques has been drawn through a commercial five-hole probe that was mounted in the same radial location as the fast response probe.

INTRODUCTION

The centrifugal compressor is commonly used in the oil and gas industry for heavy duty applications such as pipeline compression, liquefied natural gas (LNG), chemical processes and reinjection (Japikse, 1996; Cumpsty, 1989). The main reasons for its success are its reduced dimensions compared to axial machines, the intrinsic reliability of the radial compressor system, again, versus axial compressors, its fairly large operational range at fixed driver speed with no need for adjustable inlet guide vanes (IGVs), and, last but not least, to the high efficiency levels obtainable.

When turbomachinery is designed for a customer's technical specifications, the producer has to guarantee the required performance (efficiency, work coefficient and flow rate, as well as the off-design operability range). These points are often part of the purchase agreement, and are verified by testing of the machine (Tapinassi, et al., 2006).

The producer typically assembles a set of components (e.g., impeller, diffuser, inlet scroll) in a multistage arrangement. The issue of assessing the performance of each stage is an old one, and much effort has been spent, and will be spent, on increasing the

accuracy and design tool predictability (Scotti Del Greco, et al., 2007). Experimental activities are a key phase in this process. An in-depth understanding and detailed knowledge of the complex phenomena that take place along the compressor flow path is fundamental to the development and continuous improvement of the tools and codes, both 1D and computational fluid dynamics (CFD), which are employed daily in stage design.

Since reliable numerical predictability can lead to a reduction of the number of stage tests required, experimental activities in support of CFD are essential for producing results with a higher and higher resolution and accuracy. Moreover, in spite of recently enhanced numerical tool capabilities, it has become clear that—with special reference to certain stage families, e.g., those with large flow coefficients and impellers that are not purely radial—standard test outcomes may not be sufficient.

This is the scenario in which this research activity was initiated. Actually, the standard measurement techniques, employing pneumatic devices, such as the cobra and the five-hole probe, may only lead to the obtaining of time-averaged data when installed in a highly pulsating flow field; significant hypotheses and approximations are then necessary to compare such output to CFD data. To overcome this limitation, a fast response aerodynamic pressure probe (FRAPP) was installed at the exit section of a centrifugal impeller which was tested at the GE Oil & Gas Technology Laboratory.

An unsteady flow field reconstruction of total and static pressure and flow angle was obtained for different flow conditions along the same speed-line and then compared to the measurements obtained using a five-hole probe that was mounted in the same radial location as the fast response probe.

EXPERIMENTAL SETUP

The experimental work was performed at the first author's company in Florence. The test bench, whose test cell is depicted in Figure 1, consists of a closed loop rotating rig, which is employed for performance measurements of many centrifugal compressor designs; for further details (Ferrara, et al., 2006).

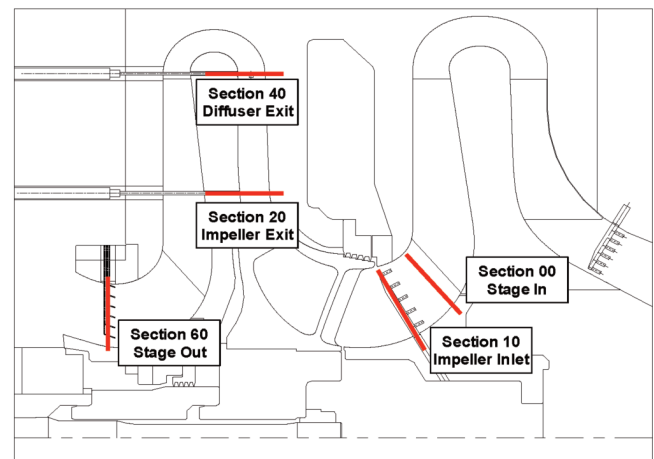


Figure 1. Test Rig Schematic.

The test campaign was carried out using air as the working gas and ambient pressure at the stage inlet. The tested impeller, referred to as Mixed Flow 956 (MF 956), which was designed for oil and gas purposes, cannot be considered purely radial since an axial velocity component, though very slight, is present at its discharge section (average pitch angle lower than ± 2 degrees). The MF 956 has 15 three-dimensional blades.

A multistage compressor was simulated through a "pseudo-stage" in the flow path upstream of the impeller. This was included in order to provide flow profiles at the impeller inlet typical of that expected in a multistage environment. The pseudo-stage consists of a set of preswirl vanes followed by a scaled version of the return channel.

The test rig was instrumented so as to allow flange-to-flange measurements, single component performance evaluation (e.g., impeller efficiency and head, diffuser recovery and losses, etc.), as well as the detection of the occurrence of stall and surge.

Measurements were taken at various locations throughout the test rig. The instrumentation used is well established and can be tailored to suit the needs of a specific study. For the purposes of this discussion, only the measurement apparatus of direct relevance to performance evaluation and FRAPP acquisition is discussed.

In accordance with the nomenclature reported in the aforementioned Figure 1, the main measurement sections are indicated as:

- Section 00: Stage inlet
- Section 10: Impeller inlet
- Section 20: Impeller outlet/diffuser inlet
- Section 40: Diffuser outlet/return channel inlet
- Section 60: Stage outlet/return channel outlet

As far as instrumentation is concerned, the measurements of total pressure were performed with Kiel probes, total temperature with shielded J-type thermocouples and flow angles either with three-hole or five-hole probes, depending on the expected three-dimensionality of the flow. At each of the measurement locations throughout the compressor, static pressure taps were positioned around the circumference of both the hub and the shroud. At the impeller inlet (Section 10), the probes were assembled as rakes and were mounted on a rotating conveyor that enabled the acquisition of high resolution measurements.

The use of multiple-probe rakes or of a single traversing probe depends to a large extent on the size of the flow channel: for narrow channels, single probes with multipoint traverses are used in order to minimize probe blockage effects on the stage performance. Moreover, probe actuators allow maximum recovery of Kiel probes and “nulling mode” operation for multihole probes for each different flow condition. Hence, downstream of the impeller and at the diffuser exit (Sections 20 and 40) axial-radial actuators were used so as to allow the traversing of total pressure, total temperature and flow angle probes. The following sections will provide more information regarding Section 20 instrumentation, where unsteady pressure measurements were performed together with the standard measurements. Finally, the stage outlet (Section 60) was instrumented with many fixed rakes to obtain a detailed flow field reconstruction.

The flow rate was measured with an orifice following the EN ISO 5167-1 standard, while the rig rotating speed was measured using a magnetic pickup based key-phaser. The uncertainties associated with the steady measurements of each section are collected in Table 1.

Table 1. Measurement Uncertainties.

Measurement	Section	Absolute Uncertainty at 95% confidence level
Temperature	10	$\pm 0.2^{\circ}\text{C}$
Pressure		$\pm 35\text{ Pa}$
Yaw Angle		$\pm 0.5\text{ deg}$
Temperature	20	$\pm 0.2^{\circ}\text{C}$
Pressure		$\pm 155\text{ Pa}$
Yaw Angle		$\pm 0.5\text{ deg}$
Pitch Angle		$\pm 0.5\text{ deg}$
Temperature	40	$\pm 0.2^{\circ}\text{C}$
Pressure		$\pm 155\text{ Pa}$
Yaw Angle		$\pm 0.5\text{ deg}$
Temperature	60	$\pm 0.2^{\circ}\text{C}$
Pressure		$\pm 155\text{ Pa}$
Yaw Angle		$\pm 0.5\text{ deg}$

FRAPP INSTALLATION

The fast response aerodynamic pressure probe, whose specification and operating details will be given in the next section, was installed at the exit section of the impeller (i.e., Section 20) in order to obtain a highly detailed flow field reconstruction. Figure 2 shows the dynamic pressure probe, while Figure 3 depicts the MF 956 impeller, captured during assembly of the test rig; the red circle shows the FRAPP location.

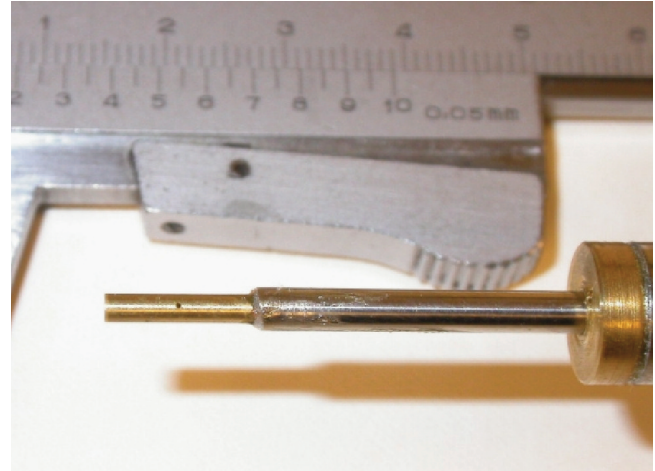


Figure 2. FRAPP Probe.

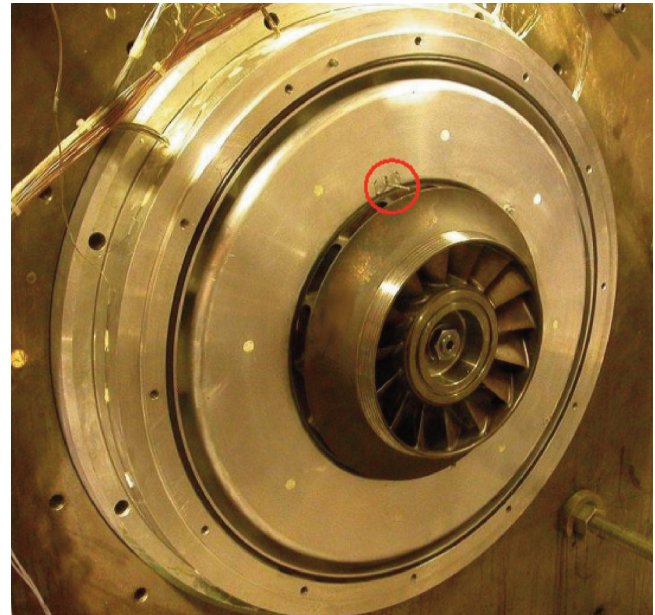


Figure 3. MF 956 Centrifugal Impeller.

Since the objectives of the present activity included a comparison of FRAPP results and measurements deriving from standard techniques, a five-hole probe was installed in the same radial location as the FRAPP, but in a different circumferential position. Unsteady measurements could then be time-averaged so as to allow a direct comparison with the pneumatic measurements, either in terms of hub-to-shroud profiles or mass averaged values in the whole section area.

FRAPP and five-hole probes were acquired at the same time and moved from the hub wall up to the shroud. Due to a smaller head dimension, FRAPP could traverse in 15 different positions, while the number of steps for the five-hole probe had to be limited to seven; refer to Figure 4, where the movement plans of the instruments are represented.

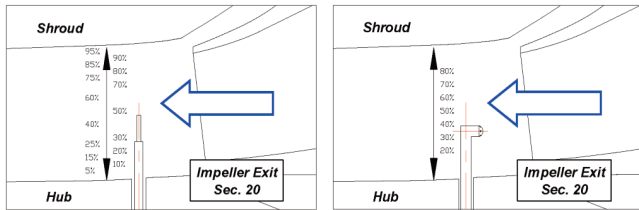


Figure 4. Movement Plan of FRAPP (Left) and Five-Hole Probe (Right).

FRAPP TECHNOLOGY AND SPECIFICATIONS

Unsteady measurement techniques for turbomachinery applications have undergone significant development in the last two decades, and are presently widely used in research test rigs. The coupling between fixed and rotating components, the highly turbulent flows, as well as the difficulties of performing measurements during rotation, make the use of time-resolved measurement techniques particularly attractive for turbomachinery. These concepts, historically conceived to support basic research, have led to mature experimental techniques, now ready for widespread industrial application.

The application of intrusive, time-resolved measurement techniques in a turbomachinery environment is not an easy task because of the small dimensions of the channels, as required in real scale industrial test rigs, and of the high frequency of the unsteady phenomena. In principle, the first problem could be significantly reduced by using scaled models of increased dimensions in similarity conditions. However such scaling, even if possible, is not used in industrial applications, and the present-day approach is to make measurements in real-scale test rigs, encouraging the miniaturization of probes. Regarding the measurement, typical rotor blade passing frequencies (BPF in the following) are in the range of 2 to 10 kHz, and, due to the steep gradients associated with flow phenomena (near wakes, strong vortices, moving shocks), five-to-10 harmonics of the BPF are needed to accurately resolve the unsteady flow downstream of a centrifugal impeller (Kupferschmied, et al., 2000).

Among the techniques available, fast response aerodynamic pressure probes represent one of the most complete and promising experimental methodologies. Thanks to miniaturization, now possible at relatively low cost, these probes combine high spatial resolution (~1 mm) and frequency response (~100 kHz), and provide information on both the pressure and the velocity fields, as well as an estimate of the turbulence level of the flow.

The FRAPP measurement concept arose from the matching of classical pneumatic directional probes and piezoresistive fast-response pressure transducers. These latter guarantee fast response, miniaturization, reliability and low cost. A wide range of different configurations is available, the most complex of which are able to measure phase-resolved (i.e., periodic) and unresolved (i.e., turbulent) total pressure, Mach number and flow angles, and time-averaged total temperature, thanks to the installation of a thermocouple in the probe head.

Three- or four-sensor fast-response probes can measure the time-resolved two- and three-dimensional flow field, but, in general, they exhibit high blockage effects. Significant miniaturization can be achieved with single-sensor probes, which allow the 2D flow field in a plane normal to the probe stem to be measured. Since the probe has only a single hole, only one measurement at a time can be performed. The flow field is then reconstructed by rearranging three pressure measurements at different angles of rotation around the probe axis, thus virtually reproducing the three-hole probe technique.

Since the measurements are taken at different times, phase-resolved measurements can be obtained by means of a phase-locked flow reconstruction, although no direct turbulence measurements can be performed. Nevertheless, some information on the turbulence level can be obtained by analyzing the measured signal at the angular position aligned to the phase-averaged flow direction. By exploiting the insensitivity of the probe head to flow angles inside ± 10

degrees, the time-resolved total pressure is measured and can be used to derive the unresolved unsteadiness. Assuming isotropic turbulence, this quantity can be linked to the turbulence level of the flow (Persico, et al., 2008).

For the aforementioned reasons, a large technical university in Milan, Italy, has been developing the single-sensor FRAPP technology over the last 10 years (Barigozzi, et al., 2000; Persico, et al., 2005a). Several FRAPPs have been designed and tested, and have been widely used in research test rigs for high pressure subsonic and transonic turbine stages (Gaetani, et al., 2007; Persico, et al., 2009; Schennach, et al., 2010).

In this paper, the first application of the university's FRAPP technology to an industrial test rig is presented. The probe considered here was developed around a commercial miniaturized pressure sensor (full scale 25 psi) to ensure high reliability, low cost and simplified manufacturing of the probe heads. The transducer is installed coaxially with the probe head to obtain a minimum probe head diameter of 2.0 mm. The final probe spatial resolution, defined as the physical distance between the extreme positions of the tap, is 1.5 mm. The single pressure tap on the probe head has a diameter of 0.3 mm.

The sensor is electrically compensated for temperature by the manufacturer to reduce thermal drift, but this setup is usually not sufficient to compensate for the temperature sensitivity of piezoresistive sensors (Dénos, 2002) entirely. Therefore, a special temperature calibration procedure was applied. In it, the probe is calibrated for different pressures and temperatures in a calibration oven, and the pressure measurements are corrected by assuming the transducer's sensitivity and offset to be linearly dependent on temperature.

Since the transducer is subsurface mounted, a line-cavity system connects the measurement environment to the sensing element. Detailed numerical techniques were used to define the probe internal geometry to enhance the probe frequency response up to 50 kHz (Persico, et al., 2005a). The dynamic characteristics of the probe were then verified on a low pressure shock tube developed for the dynamic calibration of fast-response probes (Persico, et al., 2005b; Gaetani, et al., 2008). The probe showed a resonance region at 45 kHz, but thanks to the experimental determination of the transfer function, the operational frequency range can be generally extended up to 80 to 100 kHz by means of digital compensation.

The probe aerodynamic performance was evaluated in a calibrated nozzle for Mach numbers ranging from 0.15 to 0.75. The expanded uncertainty of the pressure measurements was ± 0.5 percent of the kinetic head, and that of the flow angle was ± 0.2 degree over the calibration range (± 22.5 degrees). The angular range of the probe application (equal to ± 22.5 degrees for a defined class of three pressure values), can be extended to ± 180 degrees by eight 45 degree rotations of the probe, exploiting the virtual character of the probe operational mode.

Specific tests showed that the pressure reading of the probe is weakly sensitive to meridian flow angles (i.e., in a plane containing the probe axis) inside ± 10 degrees. The FRAPP measurement errors caused by high meridian flow angles, evaluated during the aerodynamic calibration, are reported in Table 2. Note that the probe does not exhibit a symmetrical behavior around 0 degrees.

Table 2. Errors in the FRAPP Readings Due to High Meridian Flow Angles.

Pitch Angle	Static and total pressure	Mach number	Yaw angle
-10 deg	8% of the kinetic head	0.02	0.30 deg
+10deg	1% of the kinetic head	0.01	0.15 deg

The instantaneous pressure signals were acquired at 1 MHz for a period of 1 second. Raw pressure data were phase-locked to the rotor wheel and then phase-averaged to obtain 40 intervals on a single rotor-blade passing period (BPP). The resulting physical

sample rate was ~ 137 kHz, in line with the frequency response of the system. As a final step, the flow properties were derived by the combination of the different phase-averaged pressures.

The unsteady flow quantities, originally measured in the absolute frame, were further converted into relative quantities making use of the time-averaged total temperature measured at station 20. Finally, the turbulence kinetic energy was also computed from the estimate of the unresolved unsteadiness of total pressure (Persico, et al., 2008).

The unsteady results were displayed as snapshots of the rotor passage flow field in the relative frame. Without a bladed diffuser downstream of the impeller, no blade row interaction mechanisms occur in this machine. Therefore, the snapshots can be regarded as the steady flow field detected by a relative-frame observer moving along the stream-wise coordinate from the inner to the outer radii (Figure 5). In the maps reported in the following sections, the rotor phase zero roughly corresponds to the trailing edge position (suction side) of the impeller.

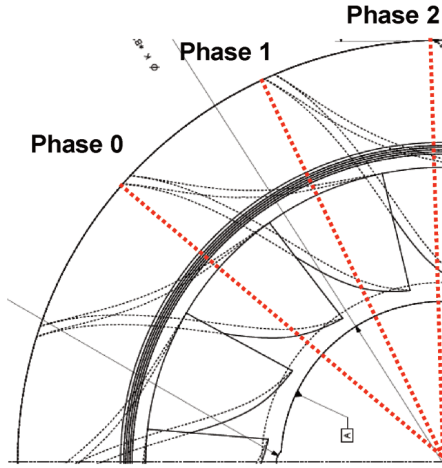


Figure 5. Reference System for Unsteady Data Representation.

EXPERIMENTAL RESULTS

Experimental results of the test campaign are reported in the next sections.

Performance Curves

Before going into a more detailed flow field analysis, a brief look at performance curves would be useful. As a standard for compressors, stage performance is evaluated as a function of flow coefficient Φ , as defined in Equation 1, which has been referenced to the design value Φ_{design} :

$$\Phi = \frac{4Q}{\pi D_2^2 u_2} ; \Phi^* = \frac{\Phi}{\Phi_{design}} \quad (1)$$

where Q is the volumetric flow rate in m^3/s , D_2 is the impeller tip diameter in m and u_2 is the impeller peripheral speed in m/s.

Since the focus of the present activity is on pressure measurements, the impeller pressure ratio (PR) was chosen as the most representative performance parameter. PR was then scaled with respect to the design point pressure ratio (i.e., PR at the nominal impeller flow coefficient):

$$PR = \frac{TP_{20}}{TP_{10}} ; PR^* = \frac{PR}{PR_{design}} \quad (2)$$

where TP_{10} and TP_{20} represent the total pressure, respectively, at the impeller inlet and outlet. The two different PR^* trends reported in Figure 6 were obtained by mass averaging the total pressure at the impeller exit measured with the five-hole probe (in black) and using FRAPP (in red).

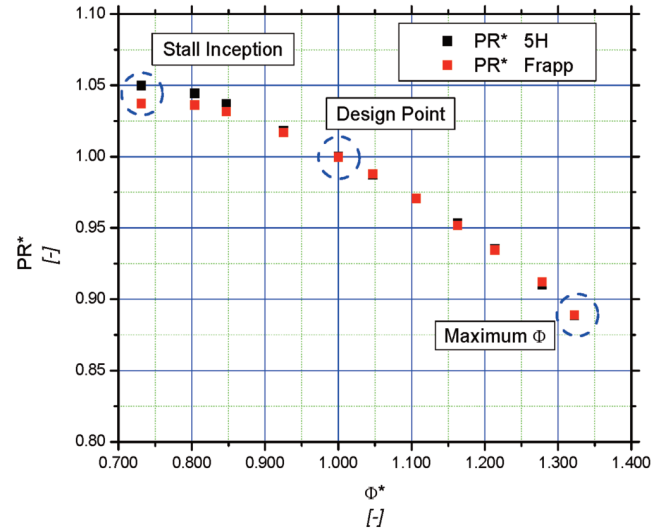


Figure 6. Pressure Ratio.

The good agreement between these different techniques is recognizable at a glance; discrepancies arise only at the lower flow rates where a highly marked jet and wake behavior is truly evident (see the next section) and instabilities may affect the flow field. Figure 7 depicts the blade-to-blade flow angle (defined from the radial direction and positive when the tangential velocity component has the same sign as the peripheral velocity) as a function of the flow coefficient; data were mass averaged over the whole flow field and referenced to a conventional angle α_{ref} . Examining this plot, the truly perfect agreement between the considered devices is once again highlighted.

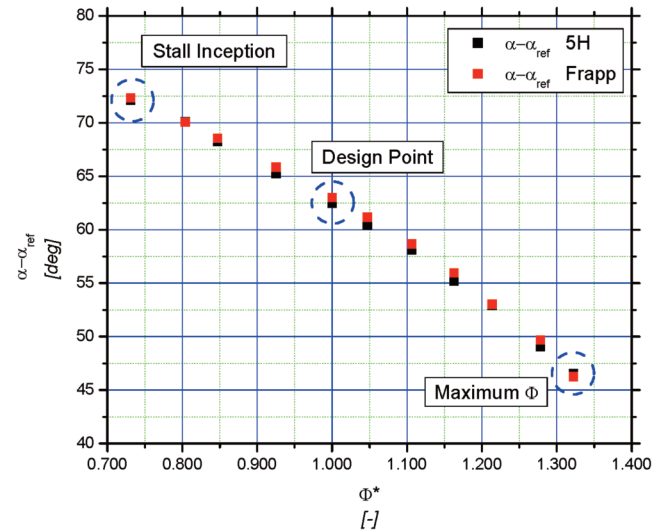


Figure 7. Yaw Angle.

So as to dig deeper into the flow field characteristics, three test points, which are representative of different behavior, were selected: the maximum flow rate condition, the design point and the inception of stall.

Flow-Field Analysis

Once the performance in terms of pressure ratio versus flow rate was highlighted, an understanding of the flow field whose averaged point lays on the performance curve is of interest. As previously noted, the FRAPP device used in this study gives information on the 2D phase-resolved flow field over the entire blade discharge section.

Consider the absolute total pressure field (in terms of the pressure ratio between sections 20 and 10) at the three selected operating points (representative of the maximum flow rate condition, the design point and stall inception) as featured in Figure 8. Here the blade span and pitch are made nondimensional and the axis origin is in the hub/blade suction side corner.

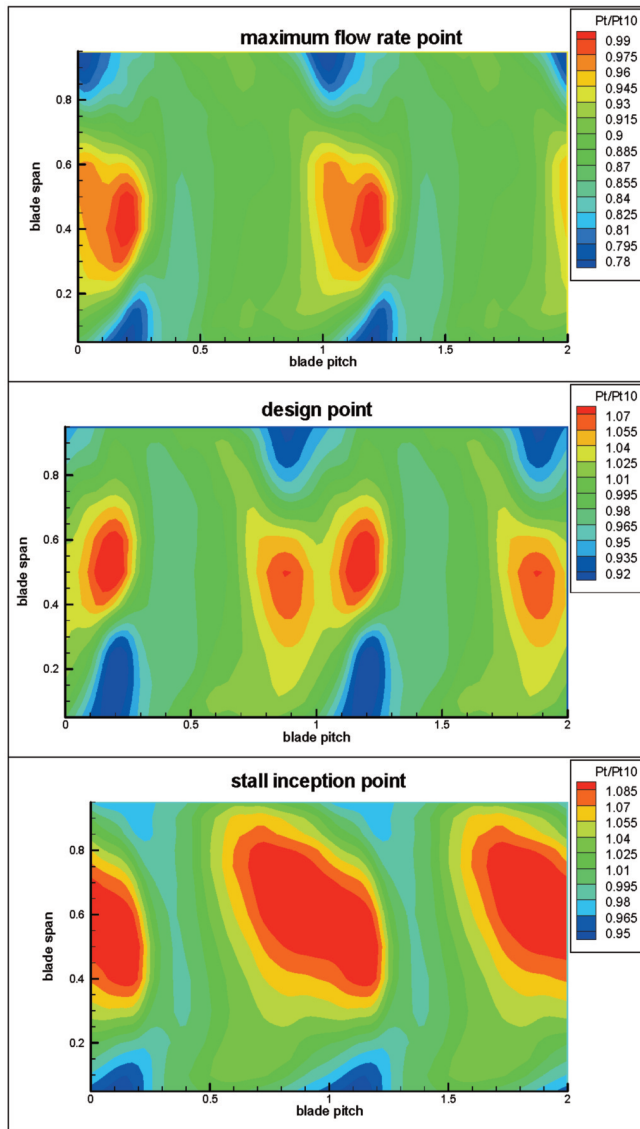


Figure 8. Total Pressure Ratio for the Three Operating Points Considered.

As reported in the image, the absolute total pressure maps evidence a highly nonuniform (and, hence, unsteady in the absolute frame of reference) pattern both along the blade span and the blade pitch for all the chosen operating points. The pattern, though at a different pressure level, is quite repetitive with a high pressure region located roughly at midspan at the same circumferential position of the blade trailing edge. The high total pressure zone is contoured by a low pressure strip along the blade span and a huge defect at some positions of the hub and tip casing. As is well known, the understanding of the absolute flow field at the impeller discharge section is of great importance for predicting and optimizing the diffuser performance. At the same time, its distribution depends on the flow field within the impeller and results from the combination of many quantities both in the relative and absolute frames of reference, which will be reported and discussed in the following.

The turbulent kinetic energy (TKE) maps (Figure 9), although derived under quite strict assumptions, provide interesting information from a qualitative point of view. In particular, the turbulent kinetic energy field evidences, regardless of the flow rate condition, a strip along the blade span of very high value with a peak at 20 to 30 percent from the hub casing. This region is connected to the blade wake that promotes turbulent flows and losses.

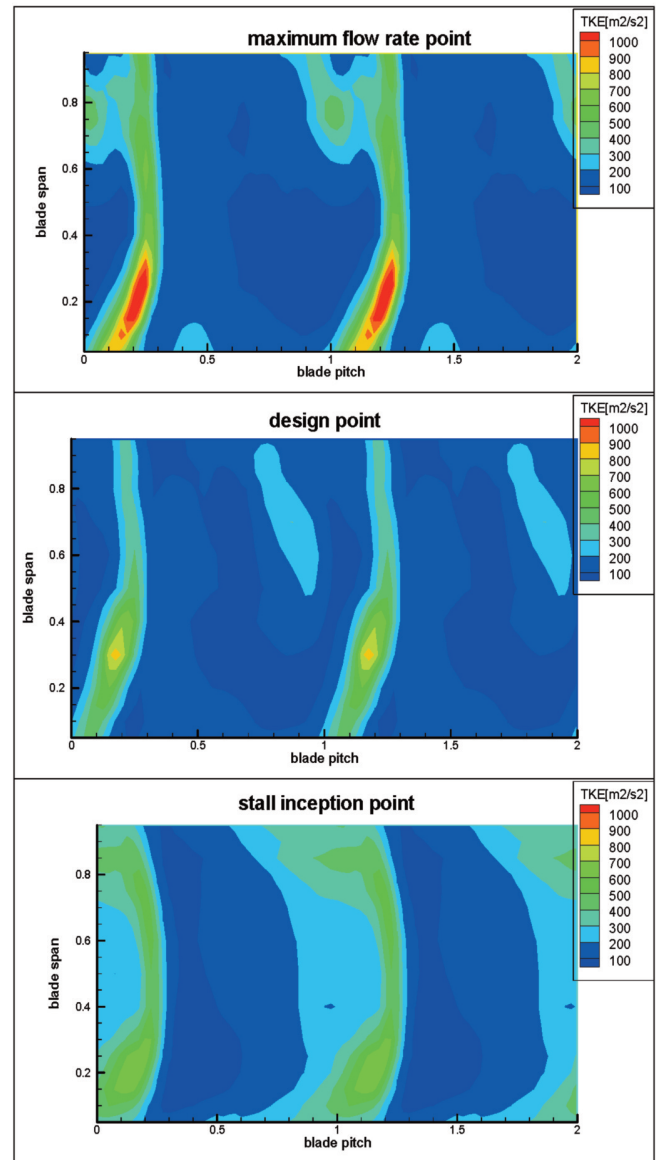


Figure 9. Turbulent Kinetic Energy for the Three Operating Points Considered.

Focusing on the maximum flow rate condition, a second region of high TKE is found at the blade tip—suction side corner. This feature, as also often evidenced by laser Doppler velocimetry (LDV) measurements in centrifugal impellers, corresponds to the result of the secondary flow and dissipation activities accumulated under the pressure field action within the impeller blade passage. As the flow rate decreases, this region moves away from the suction side region towards midpitch and spreads over the blade channel. At the inception of stall, the TKE field evidences a wide dissipation region over the blade passage that assumes an almost 2D pattern (nonuniformities are mainly in the tangential direction).

Figure 10 reports the blade-to-blade angle (ALFA) defined from the radial direction and positive when the tangential velocity component has the same sign as the peripheral velocity. The blade-to-blade angle pattern evidences the same general character of TKE with tangential flow (high ALFA value) where TKE is high, and a more radial pattern in the free-stream/isentropic regions (no shock occurs in the impeller).

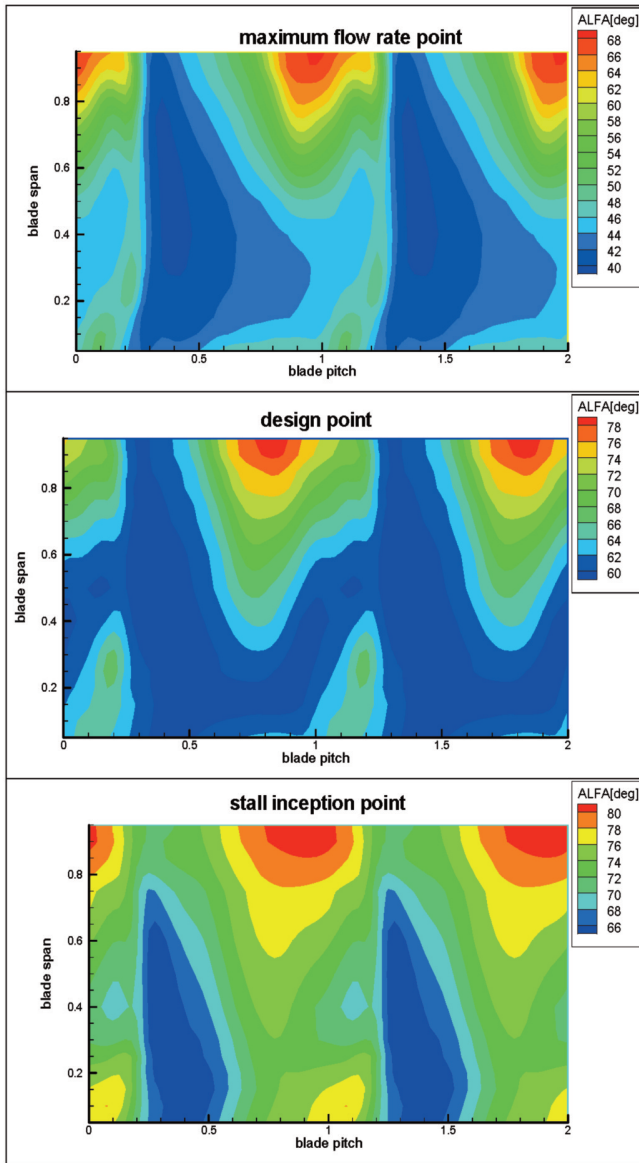


Figure 10. Blade-to-Blade Flow Angle for the Three Operating Points Considered.

Since the absolute flow field discharged by the impeller is the result of complex fluid dynamic phenomena within the impeller itself, the understanding of the flow physics requires the representation of the flow field in the relative frame of reference. Turning first to the relative Mach number commonly used to evidence the jet and wake structure of the flow, Figure 11 shows a flow field consistent with the TKE map reported in Figure 10. In fact, where TKE is high, the relative Mach number is generally low. It is interesting to observe that in the tip region, the relative Mach number defect is much higher than that measured in the blade wake at midspan. For the maximum flow rate condition, the field is not uniform along either the span or the pitch of the blade, while for the minimum flow rate, the

nonuniformity is mainly along the pitch leading to a common jet and wake structure. For the design operating point, the minimum of the relative Mach number shifts towards midpitch evidencing, in the tip region, two minima corresponding to two dissipative phenomena also evidenced in the TKE field.

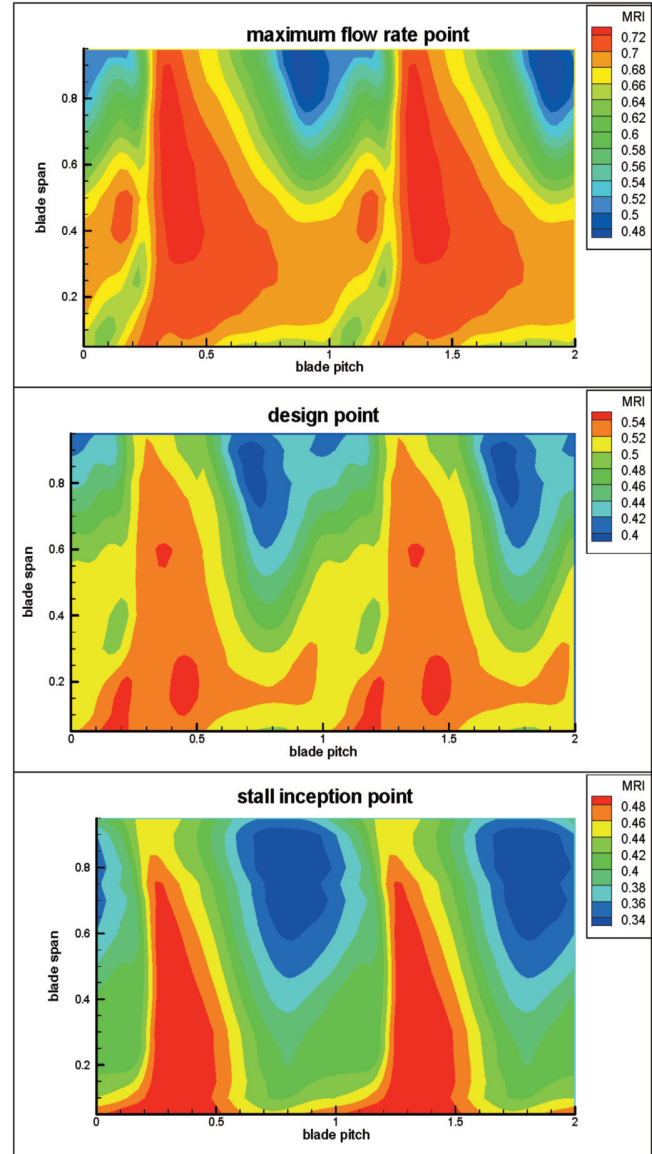


Figure 11. Relative Mach Number for the Three Operating Points Considered.

The static pressure fluctuation being of low magnitude, the relative total pressure field has the same pattern as the relative Mach number case and, hence, is not shown for the sake of brevity.

To obtain further insight into the impeller flow field, the relative flow angle in the blade-to-blade plane is reported in Figure 12; the angle is defined from the radial direction and taken as positive when it has the same orientation as the blade angle. The quantity is dominated by the jet and wake structure even if the velocity triangle composition leads to some complication in the comprehension of the maps. The flow region adjacent to the blade has a flow angle similar to the blade region (please note that for proprietary reasons, all the angular values have been shifted) while the flow region with high radial velocity has a greater slip and, hence, relative flow angle.

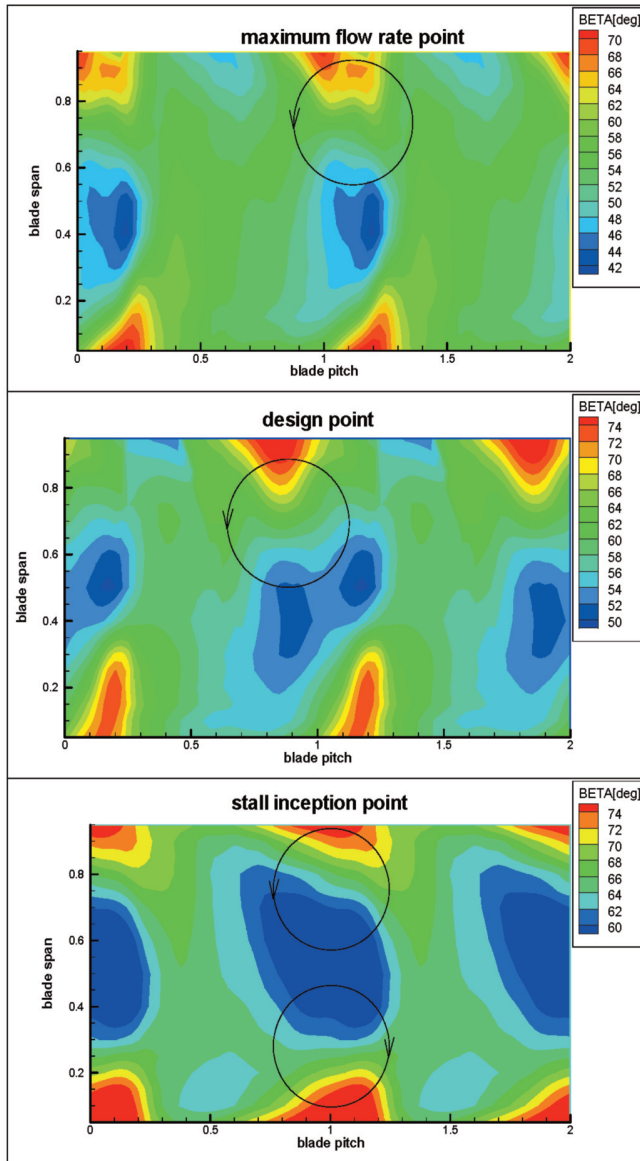


Figure 12. Relative Blade-to-Blade Flow Angle for the Three Operating Points Considered.

If the Rankine vortex model is applied to the flow field, a vortex can be observed in the tip region for all three operating conditions under consideration. According to the Rankine model, a vortex can be seen as a combination of a forced vortex in the core contoured by a free vortex. In terms of blade-to-blade angle, the vortex appears as a succession of straight contour steps in the core contoured by closed contour steps above and below the vortex core. In particular, the tip casing region shows a counterclockwise rotating vortex structure whose position, dimension and intensity varies with the flow rate.

On the contrary, in the hub region, a vortex structure can be seen only at the minimum flow rate; its sense of rotation is clockwise. All the vortex structures shown in Figure 12 are consistent with the secondary flow pattern observed concerning the impeller. The tip pattern is more developed and dissipative due to the flow phenomena occurring within the blade channel.

To get more insight from the designer perspective, the phase-resolved global quantities such as the work exchange, the slip factor and the effective power (work times flow rate in arbitrary units) are now analyzed. For the sake of brevity, only the design case results are reported in Figure 13.

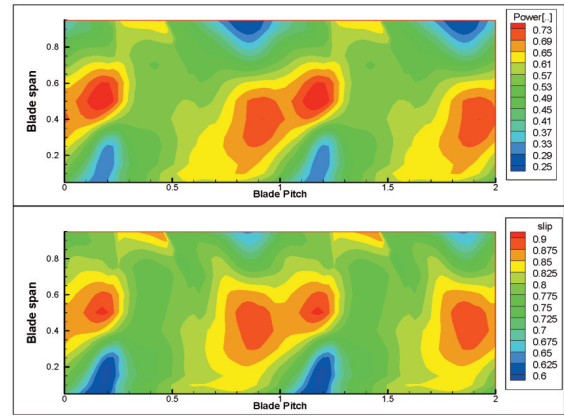


Figure 13. Effective Power and Slip Factor for the Design Operating Condition.

The slip factor is defined as follows:

$$\mu = 1 - \frac{c_{slip}}{U_2} \quad (3)$$

The slip factor and the power exchanged have roughly the same qualitative trend; to gain a worthwhile understanding, the analysis has to be carried out differently in the midspan and endwall regions. The midspan zone evidences a high slip factor in the suction side region commonly associated with the jet and wake flow character where the slip velocity is high in the jet; thanks to the low nonuniformities in the radial velocity component, the effective power is high as well. The endwall regions, on the contrary, evidence low slip factor where high tangential flows (i.e., high ALFA angle) and dissipative flows (high TKE) are encountered. In this case, the slip velocity is very high and, since it is coupled to the low flow rate associated with those regions, low effective power is transferred to the fluid.

To conclude, the availability of detailed information allows a better understanding of the flow phenomena and of their influence on the overall performance.

FRAPP—Five-Hole Probe Comparison

The average data derived from phase-resolved measurements are now compared with the five-hole probe data; the results are reported for hub to shroud trends. The test conditions considered are, again, the maximum Φ , the design point and incipient stall.

The total pressure ratio profiles (PR* as defined in Equation 2) are shown in Figure 14 and the blade-to-blade flow angle profiles are presented in Figure 15, where span = 0.00 means the hub wall, whereas span = 1.00 refers to the shroud wall.

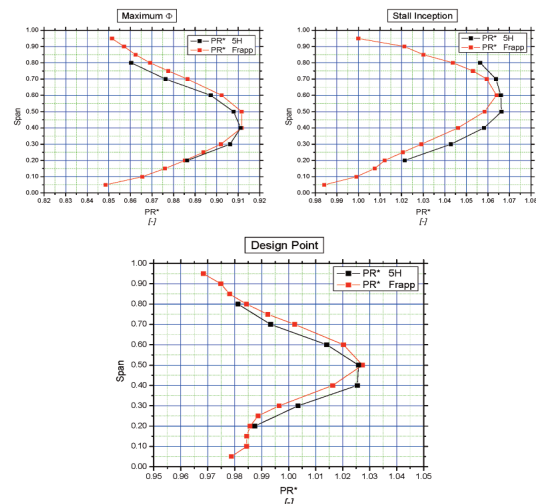


Figure 14. Total Pressure Hub-to-Shroud Profiles.

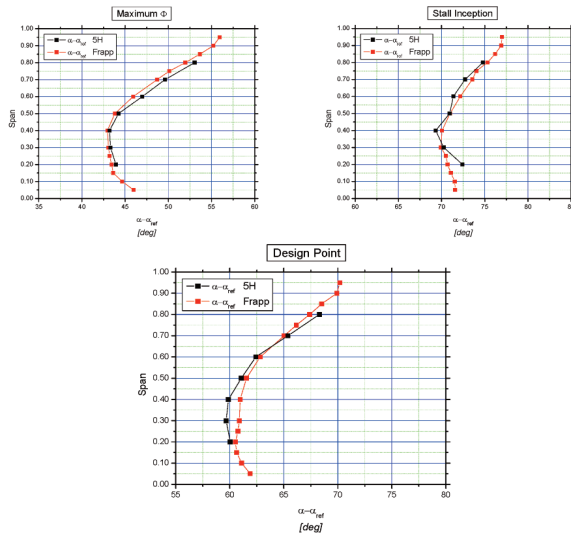


Figure 15. Yaw Angle Hub-to-Shroud Profiles.

No evident discrepancies were highlighted in the comparison of these results. Actually, even though the flow field periodically fluctuates, the flow angle fluctuation is below the calibration range of the five-hole probe. In such a context, the nulling mode procedure applied guarantees that the pneumatic probe always operates within its calibration range.

The higher differences are found in the total pressure profiles for the stall inception conditions where a significant periodic fluctuation is experienced along the entire blade height. The result appears to be consistent with a different kind of averaging occurring within the line-cavity systems of the two probes: the five-hole probe intrinsically makes a pneumatic average that is an approximation of the actual mean value of the periodic pattern. The low is the flow fluctuation, the high is the accuracy of the pneumatic average, with a relevant increase of systematic error if the flow undergoes periodic fluctuations outside the probe calibration range. Such behavior is very difficult to be foreseen theoretically, since detailed information on the flow fluctuation can be achieved only after an unsteady flow analysis is performed. Indeed, the periodic flow field is well captured by the FRAPP, and its mass-average provides a more realistic datum of the machine performance.

It is to be noted that the choice of carrying out either one of the different kinds of averaging has a limited impact on the angle detection since the five-hole probe rarely works outside its calibration range.

CONCLUSIONS

Unsteady flow field measurements were carried out at the exit section of an industrial centrifugal impeller designed for oil and gas applications. The measurements were performed using a fast response aerodynamic pressure probe (FRAPP) and the results have been thoroughly analyzed and discussed in detail.

Comparisons between the FRAPP and five-hole probe measurements, in terms of both average values over the entire flow field and hub-to-shroud profiles, have highlighted the capability of pneumatic multihole probes in rather highly pulsating flow fields when detailed information and detailed flow-field reconstruction are not required.

FRAPP measurements show flow phenomena that are consistent with the information and concepts found in the open literature. Moreover, unsteady pressure measurements, rare in the open literature where LDV or L2F measurements on centrifugal compressors are commonly reported, allow for a deep understanding of the flow phenomena in terms of pressure and, hence, in terms of losses. Another advantage of FRAPP with respect to optical techniques is that it does not require optical accesses to be

provided, usually not feasible in industrial test rigs. The high Mach number means that hot wire anemometry is not applicable due to the fragility of the measurement device. These considerations make the present FRAPP techniques undoubtedly more effective than anemometry techniques in high speed industrial test rigs. FRAPP measurements may help to improve slip factor correlations commonly applied in the design process in order to properly match the slip factor dependence on the flow rate, once the class of impellers is defined.

The detailed knowledge of the flow field entering the diffuser allows for a more effective evaluation of the mixing process that takes place within the diffuser and the diffuser efficiency itself. Furthermore, the FRAPP results allow the calibration of CFD tools applied both to impellers and diffusers either for design or analysis purposes.

One can conclude that remarkable improvements in the efficiency of both the single components and the entire compressor could be achieved by incorporating into the design process the detailed information on the flow field resulting from the application of the FRAPP measurement techniques considered in the present research paper.

REFERENCES

- Aalburg, C., Simpson, A., Schmitz, M. B., Michelassi, V., Evangelisti, S., Belardini, E., and Ballarini, V., 2008, "Design and Testing of Multistage Centrifugal Compressors with Small Diffusion Ratios," ASME Paper GT2008-51263.
- Barigozzi, G., Dossena, V., and Gaetani, P., 2000, "Development and First Application of a Single Hole Fast Response Pressure Probe," *Proceedings of the XV Symposium on Measuring Techniques in Transonic and Supersonic Flows in Turbomachines*.
- Cumpsty, N. A., 1989, *Compressor Aerodynamics*, Essex, England: Longman Scientific & Technical.
- Dénos, R., 2002, "Influence of Temperature Transients and Centrifugal Force on Fast Response Pressure Transducers," *Experiments in Fluids*, 33, pp. 256-264.
- Ferrara, G., Ferrari, L., and Baldassarre, L., 2006, "Experimental Characterization of Vaneless Diffuser Rotating Stall, Part V: Influence of Diffuser Geometry on Stall Inception and Performance (3rd Impeller Tested)," ASME Paper GT2006-90693.
- Gaetani, P., Guardone, A., and Persico, G., 2008 "Shock Tube Flows Past Partially Opened Diaphragms," *Journal of Fluid Mechanics*, 602, pp. 267-286.
- Gaetani, P., Persico, G., Dossena, V., and Osnaghi, C., 2007 "Investigation of the Flow Field in a High-Pressure Turbine Stage for Two Stator-Rotor Axial Gaps-Part II: Unsteady Flow Field," *ASME Journal of Turbomachinery*, 129, (3), pp. 580-590.
- Japikse, D., 1996, "Centrifugal Compressor Design and Performance," Concepts ETI, Inc.
- Kupferschmied, P., Koppel, P., Gizzi, W., Roduner, C., and Gyarmathy, G., 2000, "Time-Resolved Flow Measurements with a Fast-Response Aerodynamic Probe in Turbomachines," *Measurement Science and Technology*, 11, pp. 1036-1054.
- Persico, G., Gaetani, P., and Guardone, A., 2005a, "Design and Analysis of New Concept Fast-Response Pressure Probes," *Measurement Science and Technology*, 6, (9), pp. 1741-1750.
- Persico, G., Gaetani, P., and Guardone, A., 2005b, "Dynamic Calibration of Fast-Response Probes in Low-Pressure Shock Tubes," *Measurement Science and Technology*, 16, (9), pp. 1751-1759.
- Persico, G., Gaetani, P., and Osnaghi, C., 2009, "A Parametric Study of the Blade Row Interaction in a High Pressure Turbine Stage," *ASME Journal of Turbomachinery*, 131, (3), 031006.

- Persico, G., Gaetani, P., and Paradiso, B., 2008, "Estimation of Turbulence by Single-Sensor Pressure Probes," *Proceedings of the XIX Biannual Symposium on Measuring Techniques in Turbomachinery Transonic and Supersonic Flow in Cascades and Turbomachines*, Rhode-St-Genese, Belgium.
- Schennach, O., Woisetschlaeger, J., Paradiso, B., Persico, G., and Gaetani, P., 2010, "Three Dimensional Clocking Effects in a One and a Half Stage Transonic Turbine," *ASME Journal of Turbomachinery*, 132, (1), 011019.
- Scotti Del Greco, A., Biagi, F., Sassanelli, G., and Michelassi, V., 2007, "A New Slip Factor Correlation for Centrifugal Impellers in a Wide Range of Flow Coefficients and Peripheral Mach Numbers," ASME Paper GT2007-27199.
- Tapinassi, L., Fiaschi, D., and Manfrida, G., 2006, "Improving the Accuracy of Tests for Centrifugal Compressor Stage Performance Prediction," ASME ESDA International Conference on Engineering Systems Design and Analysis.